INTERNATIONAL JOURNAL FOR NUMERICAL METHODS IN FLUIDS, VOL. 13, 1251–1265 (1991)

THE INTEGRATED SINGULAR BASIS FUNCTION METHOD FOR THE STICK–SLIP AND THE DIE-SWELL PROBLEMS

GEORGIOS GEORGIOU

Unité de Mécanique Appliquée, Université Catholique de Louvain, 1348 Louvain-la-Neuve, Belgium

LORRAINE OLSON*

Department of Mathematics, Illinois Institute of Technology, Chicago, IL 60616, U.S.A.

AND

WILLIAM SCHULTZ

Department of Mechanical Engineering and Applied Mechanics, The University of Michigan, Ann Arbor, MI 48109, U.S.A.

SUMMARY

We further develop a new singular finite element method, the integrated singular basis function method (ISBFM), for the solution of Newtonian flow problems with stress singularities. The ISBFM is based on the direct subtraction of the leading local solution terms from the governing equations and boundary conditions of the original problem, followed by a double integration by parts applied to those integrals with singular contributions. The method is applied to the stick–slip and the die-swell problems and improves the accuracy of the numerical results in both cases. In the case of the die-swell problem it considerably accelerates the convergence of the free surface profile with mesh refinement. The advantages and disadvantages of the ISBFM when compared to other singular methods are also discussed.

KEY WORDS Singular basis functions Finite elements Stick–slip problem Die-swell problem

1. INTRODUCTION

In this paper we adapt a new singular finite element method (previously used for Laplace's equation[1]) to solve Newtonian flow problems with stress singularities. The accuracy and the rate of convergence of ordinary finite element methods generally become poor and very often unacceptable when a singularity is present.[2,3] The inaccuracies caused by the singularity often appear as spurious stress oscillations.[4] Mesh refinement, although commonly used, does not always adequately capture the sudden changes in the solution field and resolve the accuracy difficulties. Inaccuracies which propagate into the global solution are typically more serious. In the die-swell problem, for example, the position of the free surface depends on the mesh refinement around the singularity.[5] A coarser mesh gives more swelling and standard numerical

* Person to whom correspondence should be addressed.

0271–2091/91/201251–15$07.50

Received 20 December 1990
Revised 14 March 1991

schemes diverge if very small elements are used near the singular point. The contamination of the global solution becomes more pronounced in non-Newtonian flows, and in fact the inability to obtain results for highly viscoelastic fluids is due partially to the presence of a singularity.[6,7]

Generally speaking, singularities may often be considered to be artefacts introduced by the idealization of the physical problem or by the use of mathematical models unable to describe the physical phenomena over the entire domain (as when the continuum assumption breaks down near the walls). In some cases the singularity can be removed or at least alleviated by modifying the mathematical problem (by smoothing a corner in the geometry or by adding slip in the boundary conditions[8]). Nevertheless, the removal or the alleviation of the singularity is not always feasible or desirable, either because the singularity and/or the singular coefficients describe the global physics of the problem (as is the case in fracture mechanics and in dendrite formation, for example) or because modifications of the mathematical problem would introduce overwhelming complications.

When modification of the mathematical problem is not possible or desirable, an alternate strategy is to modify the numerical method. The exact form of the singularity is very often known from local analyses. The analyses of Michael[9] and Moffatt[10] provide the local solutions for Stokes flow near a corner formed by two walls and near the intersection of a wall and a flat free surface at any angle. Because inertial terms are negligible near walls, the leading terms of the local solution are still valid for non-zero Reynolds number flows. Holstein and Paddon[11] showed that the first three terms of the Stokesian and inertial corner flows share the same functional form. These local solutions are also valid in some viscoelastic flows whenever the Newtonian part of the stress tensor prevails near the singularity.

The incorporation of the functional form of the local solution into the numerical scheme is the basic characteristic of the various *singular* approaches implemented in a variety of numerical methods, such as finite elements, finite differences and boundary elements. As far as finite elements are concerned, one can distinguish two main categories of methods:[4]

(1) the *singular finite element method* (SFEM), in which special elements incorporating at least the radial form of the local solution (by means of special basis functions or singular geometric transformations) are employed in a small region around the singularity while ordinary elements are used in the rest of the domain
(2) the *singular basis function method* (SBFM), in which a set of supplementary basis functions chosen to reproduce the leading terms of the singularity solution is added to the ordinary finite element solution expansion.

In two previous papers[4,5] we used the SFEM to solve the stick–slip, the die-swell and the 4:1 sudden-expansion problems. It was shown that the SFEM eliminates the spurious oscillations characterizing the stresses obtained with ordinary finite elements. In the case of the die-swell problem the SFEM considerably accelerates the convergence of the free surface profile with mesh refinement.[5] As noted in Reference 4, the main drawback of the SFEM is the inability to refine the mesh extensively. With mesh refinement the singular elements become smaller in size and, consequently, the size of the region over which the singularity is given special attention is reduced. This drawback is not encountered in the SBFM owing to the fact that the singular functions are defined independently of the refinement of the underlying mesh.

In another study[12] we solved the stick–slip problem using an SBFM in which the singular basis functions were taken equal to the leading terms of the local solution multiplied by a blending function which causes the basis functions to vanish far from the singularity. We call this method the blended singular basis function method or BSBFM. The BSBFM does not introduce any additional boundary terms in the finite element formulation. The two main disadvantages include

(1) the inability to obtain good estimates for the singular coefficients (except for the first one) because the blending function creates extra terms of the same order and (2) the need for high-order integration near the singular point.[1,3] To avoid these difficulties, we have recently developed the integrated singular basis function method (ISBFM) for Laplace's equation.[1] The main characteristics of the ISBFM are the following.

1. The singular functions and the leading terms of the local asymptotic solution have the same functional form. This is useful if accurate estimates of the singular coefficients are desirable.
2. The singular functions are directly subtracted from the original problem formulation to give a modified problem with the regular (smooth) part of the solution and the singular coefficients as unknowns.
3. A double integration by parts is applied to those integrals with singular contributions to reduce them to boundary terms to be evaluated far from the singular point.
4. Lagrange multipliers are used to impose the originally essential boundary conditions.

As shown in Reference 1, the ISBFM eliminates the need for high-order integration, improves the overall accuracy and yields very accurate estimates for the singular coefficients. It also accelerates the convergence of the norm of the solution with regular mesh refinement (in accordance with theoretical error estimates) and the solution norm converges rapidly as the number of singular functions is increased.

The objective of this work is to implement the ISBFM for fluid mechanics problems to make comparisons with ordinary finite elements and the SFEM. Both the planar stick–slip and die-swell problems are considered here. The numerical results show that, when rather coarse meshes are used, the ISBFM and the SFEM give essentially the same results. Compared to ordinary finite element techniques, both methods improve the accuracy and accelerate the convergence of the free surface profile with mesh refinement in the case of the die-swell problem. However, the ISBFM can also be used with extensively refined meshes and calculates the singular coefficients directly.

The stick–slip problem is presented in detail in Section 2. Section 3 is devoted to the die-swell problem and Section 4 summarizes the conclusions.

2. THE STICK–SLIP PROBLEM

The two-dimensional geometry, governing equations and boundary conditions for the stick–slip problem are depicted in Figure 1. Assuming steady, incompressible flow and neglecting the inertia

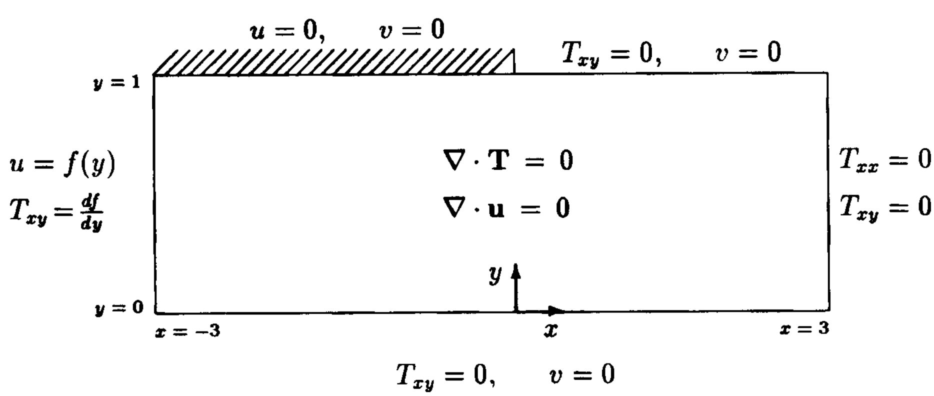

Figure 1. The stick–slip problem

and gravity effects, the momentum and continuity equations become

$$\nabla \cdot \mathbf{T} = 0, \tag{1}$$

$$\nabla \cdot \mathbf{u} = 0. \tag{2}$$

Here $\mathbf{T} = -p\mathbf{I} + \nabla\mathbf{u} + (\nabla\mathbf{u})^{\mathrm{T}}$ is the Newtonian stress tensor, $\mathbf{u}$ is the velocity vector, p is the pressure and $\mathbf{I}$ is the unit tensor. The stress components and the pressure are measured in units of $\mu U/H$, where μ is the viscosity, U is the mean velocity in the channel and H is the channel half-width. Velocity components and lengths are scaled by U and H respectively.

The local solution around the exit of the die is a special case of the steady plane flow near the intersection of a rigid boundary and a flat free surface analysed by Michael[9] and Moffatt[10] and consists of two possible solution sets. In terms of the streamfunction ψ,

$$\psi = r^{\lambda+1}\alpha_\lambda[\cos(\lambda+1)\theta - \cos(\lambda-1)\theta], \qquad \text{for } \lambda = \tfrac{1}{2}, \tfrac{3}{2}, \tfrac{5}{2}, \ldots, \tag{3}$$

$$\psi = r^{\lambda+1}\beta_\lambda[(\lambda-1)\sin(\lambda+1)\theta - (\lambda+1)\sin(\lambda-1)\theta], \quad \text{for } \lambda = 2, 3, 4, \ldots, \tag{4}$$

where (r, θ) are the plane polar co-ordinates centred at the singular point and α_λ and β_λ are constants determined from the global solution. The first term of equation (3) indicates that the stresses (including pressure) and the velocity gradients close to the singular point vary as the inverse square root of the radial distance from the exit.

2.1. Finite element formulation

The primary unknowns in our formulation are the horizontal and vertical velocity components u and v and the pressure p. In the ISBFM we directly subtract the first few terms of the local solution from the original problem formulation. In other words, we transform the mathematical problem: if (u, v, p) are the 'total' solution components and (u^s, v^s, p^s) are the singular contributions, one can write

$$u^* = u - u^s, \qquad v^* = v - v^s, \qquad p^* = p - p^s, \tag{5}$$

where (u^*, v^*, p^*) are the new unknowns corresponding to the 'smooth' part of the solution. For the singular contributions we have

$$u^s = \sum_{j=1}^{N_{\mathrm{SBF}}} \alpha_j W_u^j, \qquad v^s = \sum_{j=1}^{N_{\mathrm{SBF}}} \alpha_j W_v^j, \qquad p^s = \sum_{j=1}^{N_{\mathrm{SBF}}} \alpha_j W_p^j. \tag{6}$$

N_{SBF} is the number of singular terms subtracted from the solution, α_j are the unknown singular coefficients and W_u^j, W_v^j and W_p^j are the singular basis functions taken to be equal to the exact terms of the *odd* solution set in equation (3) (the *even* solution terms in equation (4) are regular).

By substituting equations (5) into the governing equations, the mathematical problem is transformed to that shown in Figure 2. We should stress here that (u^s, v^s, p^s) satisfy the original governing equations and the boundary conditions along the wall and the slip surface. We should also point out that instead of using essential boundary conditions for v at the inlet and at the outlet, we use natural boundary conditions.*

Now the unknown velocities $\mathbf{u}^* = (u^*, v^*)$ are expanded in terms of biquadratic basis functions (Φ^j), and the unknown pressure p^* is expanded in terms of bilinear basis functions

* The natural boundary conditions are weaker and do not require the use of Lagrange multipliers as in equation (15).

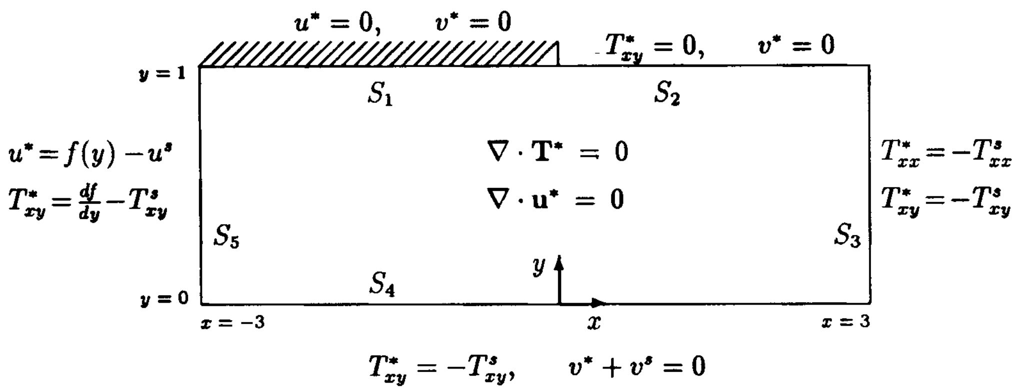

Figure 2. The modified stick–slip problem. The stars denote the new unknown variables and the superscript 's' denotes the singular contributions

(Ψ^j):

$$\mathbf{u}^* = \sum_{j=1}^{N_u} \mathbf{u}_j^* \Phi^j, \qquad p^* = \sum_{j=1}^{N_p} p_j^* \Psi^j, \tag{7}$$

where N_u and N_p are the number of velocity and pressure nodes respectively.

Applying Galerkin's principle, we weight the continuity equation by Ψ^i and the momentum equation by Φ^i:

$$\int_V \nabla \cdot \mathbf{u}^* \Psi^i \, dV = 0, \qquad i = 1, 2, \ldots, N_p, \tag{8}$$

$$\int_V \nabla \cdot \mathbf{T}^* \Phi^i \, dV = 0, \qquad i = 1, 2, \ldots, N_u, \tag{9}$$

where V is the physical domain.

To account for the additional unknown singular coefficients α_i, N_{SBF} residual equations are still required. For this purpose we add the x-momentum equation weighted by W_u^i and the y-momentum equation weighted by W_v^i to the continuity equation weighted by W_p^i. If we let

$$\mathbf{W}_u^i = (W_u^i, W_v^i),$$

then we can write

$$\int_V [(\nabla \cdot \mathbf{T}^*) \cdot \mathbf{W}_u^i + \nabla \cdot \mathbf{u}^* W_p^i] \, dV = 0, \qquad i = 1, 2, \ldots, N_{SBF}. \tag{10}$$

After applying the divergence theorem, the residual equations (9) and (10) become

$$\int_S \mathbf{n} \cdot \mathbf{T}^* \Phi^i \, dS - \int_V \mathbf{T}^* \cdot \nabla \Phi^i \, dV = 0, \qquad i = 1, 2, \ldots, N_u, \tag{11}$$

$$\int_S (\mathbf{n} \cdot \mathbf{T}^*) \cdot \mathbf{W}_u^i \, dS - \int_V (\mathbf{T}^* : \nabla \mathbf{W}_u^i - \nabla \cdot \mathbf{u}^* W_p^i) \, dV = 0, \qquad i = 1, 2, \ldots, N_{SBF}, \tag{12}$$

where S is the boundary of V. Equation (12) can be simplified further if we apply the divergence theorem once again:

$$\int_S (\mathbf{n}\cdot\mathbf{T}^*)\cdot\mathbf{W}_u^i\,\mathrm{d}S - \int_S (\mathbf{n}\cdot\mathbf{T}^{Si})\cdot\mathbf{u}^*\,\mathrm{d}S + \int_V [\mathbf{u}^*\cdot(\nabla\cdot\mathbf{T}^{Si}) + p^*\nabla\cdot\mathbf{W}_u^i]\,\mathrm{d}V = 0, \qquad i = 1, 2, \ldots, N_{\mathrm{SBF}}. \tag{13}$$

$\mathbf{T}^{Si}$ is the contribution of the ith singular functions to the stress tensor (e.g. $T_{xx}^{Si} = -W_p^i + 2\partial W_u^i/\partial x$, etc.). The volume integral of equation (13) is zero because the singular functions satisfy the original governing equations. Therefore the residual equation is reduced to a surface integral:

$$\int_S [(\mathbf{n}\cdot\mathbf{T}^*)\cdot\mathbf{W}_u^i - (\mathbf{n}\cdot\mathbf{T}^{Si})\cdot\mathbf{u}^*]\,\mathrm{d}S = 0, \qquad i = 1, 2, \ldots, N_{\mathrm{SBF}}. \tag{14}$$

As discussed above, the reduction of the volume integrals involving singular terms to boundary integrals eliminates the need to use high-order integration in the vicinity of the singular point. Notice that there is no boundary contribution on either the wall or the slip surface since the singular functions satisfy the conditions along these boundaries.

Let us now examine the boundary terms in more detail. As shown in Figure 2, the boundary S consists of five parts: (a) the wall S_1, (b) the slip surface S_2, (c) the outlet plane S_3, (d) the midplane S_4 and (e) the inlet plane S_5. The boundary terms along the wall (S_1) are ignored because essential boundary conditions for u^* and v^* are to be used. Along the slip surface (S_2) the x-direction components of the boundary terms are zero since $T_{xy}^* = T_{xy}^S = 0$. The y-direction components are ignored because of the essential boundary condition for v^*.

To impose the conditions $v^* + v^s = 0$ along S_4 and $u^* + u^s = f(y)$ along S_5, we use Lagrange multipliers[13] λ_v and λ_u respectively. These Lagrange multipliers are expanded in terms of quadratic basis functions M^j:

$$\lambda_u = \sum_{j=1}^{N_y} \lambda_u^j M^j, \qquad \lambda_v = \sum_{j=1}^{N_x} \lambda_v^j M^j, \tag{15}$$

where N_x and N_y are the numbers of nodes along S_4 and S_5 respectively. Using Lagrange multipliers introduces $N_y + N_x$ new unknowns (λ_u^j and λ_v^j) into the system. These unknowns along with the singular coefficients are introduced by means of $N_x + N_y + N_{\mathrm{SBF}}$ pseudonodes with one degree of freedom each. The nodes and pseudonodes for the first element (lower left corner of the domain) are shown in Figure 3.

The boundary term of equation (11) becomes

$$\int_S \mathbf{n}\cdot\mathbf{T}^*\Phi^i\,\mathrm{d}S = \hat{\mathbf{x}}\left(-\int_{S_3} T_{xx}^S\Phi^i\,\mathrm{d}y + \int_{S_4} T_{xy}^S\Phi^i\,\mathrm{d}x - \int_{S_5}\lambda_u\Phi^i\,\mathrm{d}y\right) + \hat{\mathbf{y}}\left[-\int_{S_3} T_{xy}^S\Phi^i\,\mathrm{d}y - \int_{S_4}\lambda_v\Phi^i\,\mathrm{d}x + \int_{S_5}\left(T_{xy}^S - \frac{\mathrm{d}f}{\mathrm{d}y}\right)\Phi^i\,\mathrm{d}y\right]. \tag{16}$$

Similarly for the two terms of equation (14) we have

$$\int_S (\mathbf{n}\cdot\mathbf{T}^*)\cdot\mathbf{W}_u^i\,\mathrm{d}S = -\int_{S_3} T_{xx}^S W_u^i\,\mathrm{d}y + \int_{S_4} T_{xy}^S W_u^i\,\mathrm{d}x - \int_{S_5}\lambda_u W_u^i\,\mathrm{d}y - \int_{S_3} T_{xy}^S W_v^i\,\mathrm{d}y - \int_{S_4}\lambda_v W_v^i\,\mathrm{d}x + \int_{S_5}\left(T_{xy}^S - \frac{\mathrm{d}f}{\mathrm{d}y}\right)W_v^i\,\mathrm{d}y. \tag{17}$$

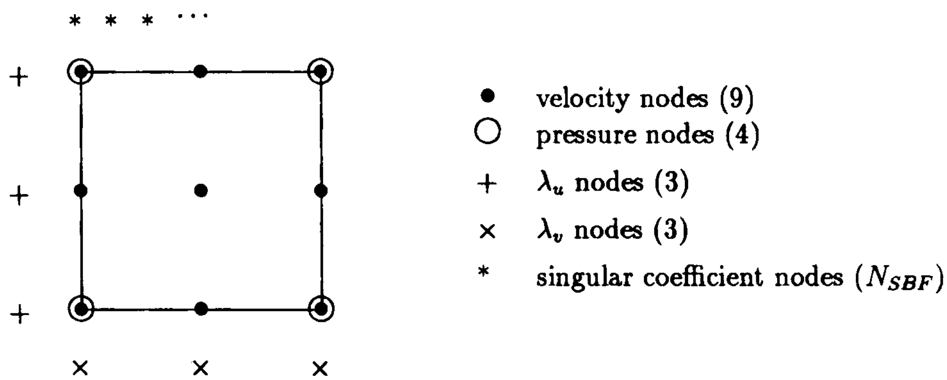

Figure 3. Nodes and pseudonodes in the first element. The number of degrees of freedom is $28+N_{\mathrm{SBF}}$

$$\int_S (\mathbf{n}\cdot\mathbf{T}^{Si})\cdot\mathbf{u}^*\,\mathrm{d}S = \int_{S_3}(u^* T^{Si}_{xx} + v^* T^{Si}_{xy})\,\mathrm{d}y - \int_{S_4}(u^* T^{Si}_{xy} + v^* T^{Si}_{yy})\,\mathrm{d}x$$
$$- \int_{S_5}(u^* T^{Si}_{xx} + v^* T^{Si}_{xy})\,\mathrm{d}y. \tag{18}$$

The final forms of the residual equations are listed below.

Continuity equations

$$\int_V \left(\frac{\partial u^*}{\partial x} + \frac{\partial v^*}{\partial y}\right)\Psi^i\,\mathrm{d}x\,\mathrm{d}y = 0, \quad i = 1, 2, \ldots, N_p. \tag{19}$$

Momentum equations

$$-\int_V \left(T^*_{xx}\frac{\partial\Phi^i}{\partial x} + T^*_{xy}\frac{\partial\Phi^i}{\partial y}\right)\mathrm{d}x\,\mathrm{d}y - \int_{S_3} T^{\mathrm{S}}_{xx}\Phi^i\,\mathrm{d}y + \int_{S_4} T^{\mathrm{S}}_{xy}\Phi^i\,\mathrm{d}x$$
$$- \int_{S_5}\lambda_u\Phi^i\,\mathrm{d}y = 0, \quad i = 1, 2, \ldots, N_{\mathbf{u}}, \tag{20}$$

$$-\int_V \left(T^*_{xy}\frac{\partial\Phi^i}{\partial x} + T^*_{yy}\frac{\partial\Phi^i}{\partial y}\right)\mathrm{d}x\,\mathrm{d}y - \int_{S_3} T^{\mathrm{S}}_{xy}\Phi^i\,\mathrm{d}y - \int_{S_4}\lambda_v\Phi^i\,\mathrm{d}x + \int_{S_5} T^{\mathrm{S}}_{xy}\Phi^i\,\mathrm{d}y$$
$$= \int_{S_5}\frac{\mathrm{d}f}{\mathrm{d}y}\Phi^i\,\mathrm{d}y, \quad i = 1, 2, \ldots, N_{\mathbf{u}}. \tag{21}$$

Singular coefficient equations

$$-\int_{S_3} T^{\mathrm{S}}_{xx} W^i_u\,\mathrm{d}y + \int_{S_4} T^{\mathrm{S}}_{xy} W^i_u\,\mathrm{d}x - \int_{S_5}\lambda_u W^i_u\,\mathrm{d}y - \int_{S_3} T^{\mathrm{S}}_{xy} W^i_v\,\mathrm{d}y - \int_{S_4}\lambda_v W^i_v\,\mathrm{d}x$$
$$+ \int_{S_5} T^{\mathrm{S}}_{xy} W^i_v\,\mathrm{d}y - \int_{S_3}(u^* T^{Si}_{xx} + v^* T^{Si}_{xy})\,\mathrm{d}y + \int_{S_4}(u^* T^{Si}_{xy} - v^{\mathrm{S}} T^{Si}_{yy})\,\mathrm{d}x$$
$$+ \int_{S_5}(-u^{\mathrm{s}} T^{Si}_{xx} + v^* T^{Si}_{xy})\,\mathrm{d}y = -\int_{S_5}\left(f T^{Si}_{xx} - \frac{\mathrm{d}f}{\mathrm{d}y} W^i_v\right)\mathrm{d}y, \quad i = 1, 2, \ldots, N_{\mathrm{SBF}}. \tag{22}$$

Lagrange multiplier equations

$$-\int_{S_4} (v^* + v^s) M^i \, dx = 0, \qquad i = 1, 2, \ldots, N_x, \tag{23}$$

$$-\int_{S_5} (u^* + u^S) M^i \, dy = -\int_{S_5} f M^i \, dy, \quad i = 1, 2, \ldots, N_y. \tag{24}$$

Notice that use of the essential boundary conditions along S_4 and S_5 was made in order to preserve the symmetry of the stiffness matrix. Equations (19)–(24) constitute a symmetric system of linear equations which is solved by a frontal solver.[14,15] The total number of unknowns is $N = N_p + 2N_u + N_{SBF} + N_x + N_y$.

2.2. *Results and discussion*

In order to make comparisons with the ordinary and singular finite element results of Reference 12, we used the same uniform meshes: mesh I with 12 × 2 elements, mesh II with 24 × 4 elements and mesh III with 48 × 8 elements. The meshes extend upstream and downstream to a distance equal to three channel half-widths to adequately approximate the inflow and outflow boundary conditions.

Results have been obtained for various values of N_{SBF} with the three meshes. Far from the singular point the ISBFM gives essentially the same results as the ordinary elements (and the singular elements as well). The estimates for the first five coefficients are listed in Table I. We observe that the first coefficient α_1 appears to approach the analytical value of 0·69099 as

Table I. Computed leading coefficients for the stick–slip problem with the ISBFM. The analytical value for α_1 is 0·69099

Mesh	N_{SBF}	α_1	α_2	α_3	α_4	α_5
12 × 2	1	0·72441				
	2	0·68716	0·29308			
	3	0·68504	0·30965	−0·00532		
	4	0·70775	0·12881	−0·01918	0·00265	
	5	0·69302	0·24592	−0·00990	0·00057	0·00004
	10	0·69327	0·24364	−0·00950	0·00047	−0·00002
	20	0·69299	0·24390	−0·00903	−0·00009	−0·00014
24 × 4	1	0·70762				
	2	0·68979	0·28261			
	3	0·68945	0·28787	−0·00451		
	4	0·68820	0·30816	0·00173	−0·00090	
	5	0·69151	0·25430	−0·01388	0·00061	0·00008
	10	0·69143	0·25561	−0·01247	0·00045	0·00002
	20	0·69138	0·25604	−0·01171	0·00001	−0·00009
48 × 8	1	0·69929				
	2	0·69064	0·27457			
	3	0·69058	0·27658	−0·00400		
	4	0·69048	0·27984	−0·00140	−0·00035	
	5	0·69112	0·25884	−0·01661	0·00064	0·00012
	10	0·69105	0·26096	−0·01365	0·00041	0·00003
	20	0·69104	0·26140	−0·01263	0·00000	−0·00008

the mesh is refined or as N_{SBF} increases. A similar trend is also observed for the other leading coefficients.

Table II compares the values of the first three coefficients with results from the literature. The calculated value of the second coefficient compares well with the value found by Ingham and Kelmanson[16] who used a singular boundary element method. With the BSBFM a satisfactory estimate is obtained only for the first coefficient, because the blending function introduces extra higher-order terms not satisfying the governing equation.[1] We should note that the singular coefficients are not directly calculated with the singular finite element method nor with ordinary finite element techniques. A least-squares fit of the velocity on the slip surface velocity was used for this purpose.[4]

As in Reference 4, the normal stress along the wall and the slip surface was used for comparisons. It is the only non-singular stress component and thus offers a severe test for the numerical calculations. The normal stresses with mesh I and $N_{SBF} = 1$ and 5 are plotted in Figure 4. Compared to the ordinary element solution, the oscillations have been essentially eliminated. As N_{SBF} increases, the normal stress becomes smoother.

Table II. Estimates of the first three coefficients for the stick–slip problem obtained with mesh III and $N_{SBF} = 5$ (only for ISBFM and BSBFM)

Method	α_1	α_2	α_3
Analytical solution[19]	0·69099	—	—
ISBFM (this work)	0·69112	0·25884	−0·01662
BSBFM[12,17]	0·69060	0·07712	0·01498
Singular elements[4]	0·69173	0·27168	0·05013
Ordinary elements[4]	0·67170	0·19812	−0·02297
Boundary elements[16]	0·69108	0·26435	0·04962

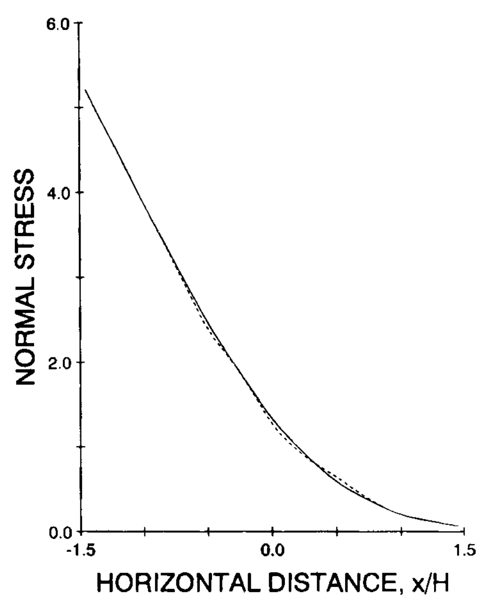

Figure 4. Normal stresses with mesh I: – – –, $N_{SBF} = 1$; ——, $N_{SBF} = 5$

The normal stresses with meshes I and III and $N_{SBF} = 1$ are plotted in Figure 5. In contrast to the SFEM,[4] the small-amplitude oscillations in the normal stress diminish as the mesh is refined. This is illustrated in Figure 6, where we compare the results of the two methods obtained using a refined mesh (mesh V from Reference 4). However, the singular elements give more accurate results with coarse meshes.

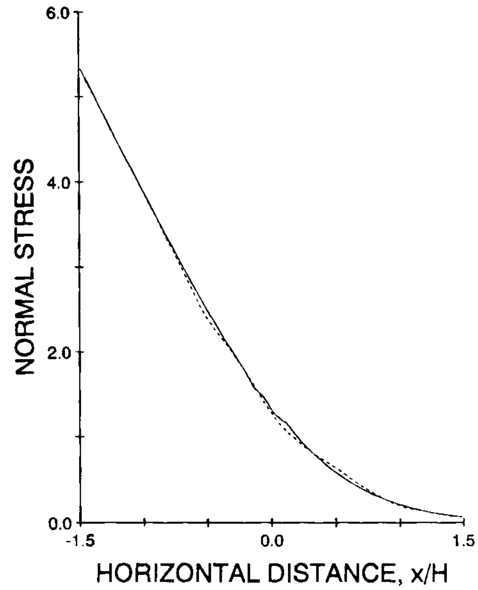

Figure 5. Normal stresses $N_{SBF}=1$: – – –, mesh I; ——, mesh III

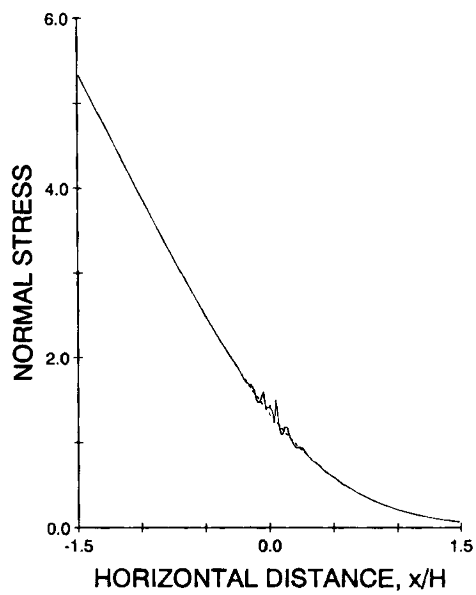

Figure 6. Comparison of the normal stresses obtained with the ISBFM (– – –, $N_{SBF}=1$) and the SFEM (——) using a refined mesh

3. THE DIE-SWELL PROBLEM

The geometry, governing equations and boundary conditions for the die-swell problem are illustrated in Figure 7. The equations and boundary conditions are the same as those of the stick–slip problem except along the free surface, the position of which is unknown. We must simultaneously satisfy three conditions on the free surface.

1. No fluid flows through the free surface (the kinematic condition):
$$\mathbf{n}\cdot\mathbf{u}=0, \tag{25}$$
where $\mathbf{n}$ is the unit normal vector pointing outwards from the free surface.
2. The shear stress is zero:
$$\mathbf{nt}:\mathbf{T}=0, \tag{26}$$
where $\mathbf{t}$ is the unit tangential vector.
3. The normal stress balances the capillary pressure:
$$\mathbf{nn}:\mathbf{T}=2H/Ca, \tag{27}$$
where $2H$ is the mean curvature of the free surface and $Ca\equiv\mu U/\sigma$, σ being the surface tension.

The kinematic equation provides the additional equation needed to calculate the unknown free surface profile $h(x)$; the other two equations serve as boundary conditions for the momentum equation. Notice that the die-swell problem is non-linear owing to the presence of the unknown free surface.

3.1. Finite element formulation

To implement the ISBFM, we use the singular functions developed for the stick–slip problem. In the infinite-surface-tension limit of the die-swell problem we recover the stick–slip problem. In the zero-surface-tension limit the use of the same functions is jutified by Michael's analysis[9] which

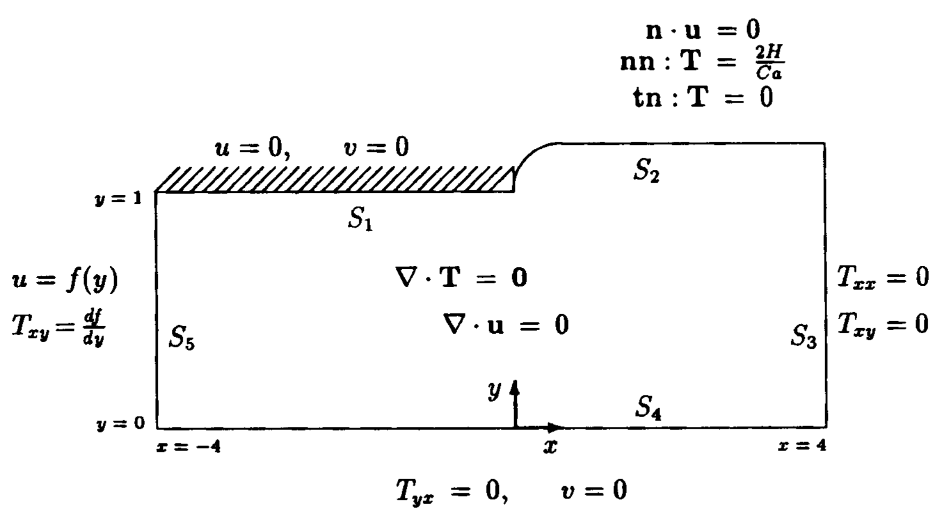

Figure 7. The die-swell problem

shows that the angle between the wall and a free surface must be 180°. Obviously, the singular functions do not satisfy the boundary conditions everywhere along the free surface (except in the infinite-surface-tension case) and therefore additional boundary terms along S_2 appear in the finite element formulation.

Full Newton iteration is employed here to compute the free surface profile simultaneously with the velocity and pressure fields, as in the ordinary finite element method and SFEM.[12,17] Quadratic basis functions M^i are used to expand the free surface location and to weight the kinematic equation. The mesh is updated at each iteration step according to the new position of the free surface. More details about the method are given in Reference 17.

The final forms of the continuity and Lagrange multiplier equations are the same as those of the stick–slip problem. The momentum, singular coefficient and kinematic residual equations are now given as follows.

Momentum equations

$$-\int_V\left(T^*_{xx}\frac{\partial\Phi^i}{\partial x}+T^*_{xy}\frac{\partial\Phi^i}{\partial y}\right)\mathrm{d}x\,\mathrm{d}y-\frac{1}{Ca}\int_{S_2}\frac{1-\sqrt{(1+h_x^2)}}{\sqrt{(1+h_x^2)}}\frac{\partial\Phi^i}{\partial x}\mathrm{d}x-\int_{S_2}(-h_xT^{\mathrm{S}}_{xx}+T^{\mathrm{S}}_{xy})\Phi^i\,\mathrm{d}x$$
$$-\int_{S_3}T^{\mathrm{S}}_{xx}\Phi^i\,\mathrm{d}y+\int_{S_4}T^{\mathrm{S}}_{xy}\Phi^i\,\mathrm{d}x-\int_{S_5}\lambda_u\Phi^i\,\mathrm{d}y=0,\quad i=1,2,\ldots,N_{\mathbf{u}},\tag{28}$$

$$-\int_V\left(T^*_{xy}\frac{\partial\Phi^i}{\partial x}+T^*_{yy}\frac{\partial\Phi^i}{\partial y}\right)\mathrm{d}x\,\mathrm{d}y-\frac{1}{Ca}\int_{S_2}\frac{h_x}{\sqrt{(1+h_x^2)}}\frac{\partial\Phi^i}{\partial x}\mathrm{d}x-\int_{S_2}(T^{\mathrm{S}}_{yy}-h_xT^{\mathrm{S}}_{xy})\Phi^i\,\mathrm{d}x$$
$$-\int_{S_3}T^{\mathrm{S}}_{xy}\Phi^i\,\mathrm{d}y-\int_{S_4}\lambda_v\Phi^i\,\mathrm{d}x+\int_{S_5}T^{\mathrm{S}}_{xy}\Phi^i\,\mathrm{d}y=\int_{S_5}\frac{\mathrm{d}f}{\mathrm{d}y}\Phi^i\,\mathrm{d}y,\quad i=1,2,\ldots,N_{\mathbf{u}}.\tag{29}$$

Singular coefficient equations

$$-\frac{1}{Ca}\int_{S_2}\frac{1-\sqrt{(1+h_x^2)}}{\sqrt{(1+h_x^2)}}\frac{\partial W^i_u}{\partial x}\mathrm{d}x-\frac{1}{Ca}\int_{S_2}\frac{h_x}{\sqrt{(1+h_x^2)}}\frac{\partial W^i_v}{\partial x}\mathrm{d}x$$
$$-\int_{S_2}[(-h_xT^{\mathrm{S}}_{xx}+T^{\mathrm{S}}_{xy})W^i_u+(T^{\mathrm{S}}_{yy}-h_xT^{\mathrm{S}}_{xy})W^i_v]\,\mathrm{d}x-\int_{S_3}T^{\mathrm{S}}_{xx}W^i_u\,\mathrm{d}y+\int_{S_4}T^{\mathrm{S}}_{xy}W^i_u\,\mathrm{d}x$$
$$-\int_{S_5}\lambda_uW^i_u\,\mathrm{d}y-\int_{S_3}T^{\mathrm{S}}_{xy}W^i_v\,\mathrm{d}y-\int_{S_4}\lambda_vW^i_v\,\mathrm{d}x+\int_{S_5}T^{\mathrm{S}}_{xy}W^i_v\,\mathrm{d}y-\int_{S_3}(u^*T^{\mathrm{S}i}_{xx}+v^*T^{\mathrm{S}i}_{xy})\,\mathrm{d}y$$
$$+\int_{S_4}(u^*T^{\mathrm{S}i}_{xy}-v^{\mathrm{s}}T^{\mathrm{S}i}_{yy})\,\mathrm{d}x+\int_{S_5}(-u^{\mathrm{s}}T^{\mathrm{S}i}_{xx}+v^*T^{\mathrm{S}i}_{xy})\,\mathrm{d}y$$
$$=-\int_{S_5}\left(fT^{\mathrm{S}i}_{xx}-\frac{\mathrm{d}f}{\mathrm{d}y}W^i_v\right)\mathrm{d}y,\quad i=1,2,\ldots,N_{\mathrm{SBF}}.\tag{30}$$

Kinematic equations

$$\int_{S_2}[(-h_xu^*+v^*)+(-h_xu^{\mathrm{s}}+v^{\mathrm{s}})]\,M^i\,\mathrm{d}x=0,\quad i=1,2,\ldots,N_h.\tag{31}$$

N_h is the number of the unknown free surface nodes. Thus the total number of unknowns is now $N=N_p+2N_{\mathbf{u}}+N_{\mathrm{SBF}}+N_x+N_y+N_h$. Details about the treatment of the integrals along the free surface are given elsewhere.[17]

3.2. Results and discussion

In order to make comparisons, we use three meshes of different refinement (I, II and III) which we used previously in studying ordinary finite elements and the SFEM.[5] All meshes extend four channel half-widths upstream and downstream. The converged meshes are shown in Figure 8 and their characteristics are listed in Table III.

The obvious choice for comparisons is the free surface profile. In Figure 9 we compare the free surface profiles for zero surface tension predicted with the ordinary finite elements, using all meshes, and the ISBFM solution obtained with the coarsest mesh I and one singular function ($N_{SBF}=1$). The ISBFM gives essentially identical results for the free surface position and the die-swell ratio for all meshes (see Table IV), so we have not plotted the free surface profile for mesh II or III here. As shown in Figure 9, the free surface profiles obtained with the ordinary finite elements converge slowly to the ISBFM result. Clearly, the ISBFM accelerates the convergence of the free surface profile with mesh refinement.

With $N_{SBF}=1$ the singular coefficient for the three meshes shows more variation than the free surface position: with mesh I $\alpha_1=0{\cdot}682$, with mesh II $\alpha_1=0{\cdot}701$ and with mesh III $\alpha_1=0{\cdot}715$. The non-linear iteration seems quite sensitive to the value of the singular coefficient, and in fact with

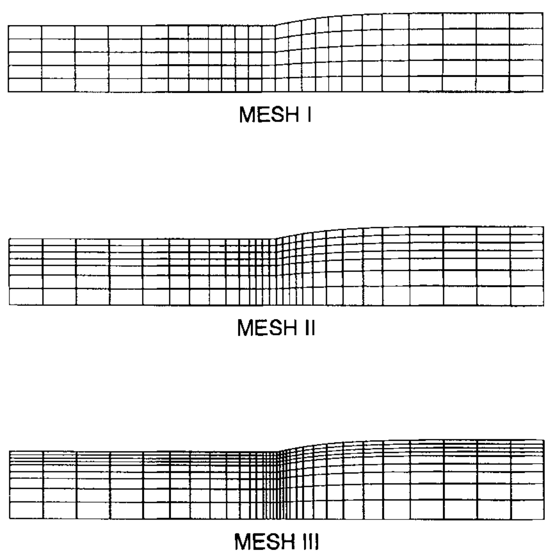

Figure 8. Converged ISBFM meshes for the die-swell problem at zero surface tension

Table III. Data for the meshes used for the die-swell problem

Mesh	Number of elements	Number of nodes	Degrees of freedom	Size of corner elements
I	120	600	1314	0·20
II	196	928	2044	0·10
III	288	1320	2918	0·10

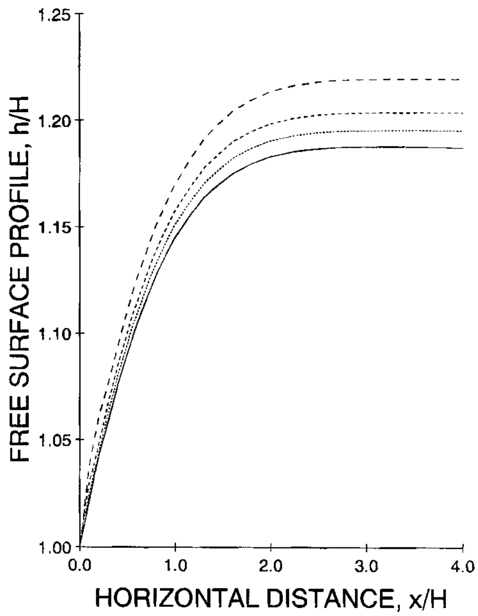

Figure 9. Computed free surface profiles at zero surface tension: – – –, ordinary mesh I; - - - - - -, ordinary mesh II; ········, ordinary mesh III; ———, singular mesh I

Table IV. Predicted die-swell ratios with ordinary elements, the SFEM and the ISBFM

Mesh	Ordinary elements	SFEM	ISBFM
I	1·2193	1·1865	1·1871
II	1·2036	1·1863	1·1866
III	1·1952	1·1860	1·1864

more than one singular function the iteration diverges for some values of Ca (particularly for $Ca > 1$). We feel that this is due to the strength of the singular contributions on the free surface.

As reported in Reference 5, the acceleration of convergence for the free surface profile with mesh refinement is also achieved with the SFEM. The SFEM is relatively simple to implement because no extra boundary terms appear in the formulation and it does not require knowledge of the angular form of the asymptotic functions. However, the SFEM performs poorly on extensively refined meshes since the singular elements also become small.

It should be noted that the free surface slope at the origin is not zero and hence violates the separation condition of Michael[9] for flows with zero surface tension. Schultz and Gervasio[18] conjecture that the free surface has infinite curvature at the singular point. We have not yet implemented singular shape functions in addition to singular basis functions; however, the slope at the origin appears to decrease as the mesh is refined.

4. CONCLUSIONS

The integrated singular basis function method (ISBFM) was used to solve the stick–slip and the die-swell problems. Compared to ordinary finite elements, the method eliminates the oscillations that characterize the normal stress along the wall and the position of the free surface. In the case of the die-swell problem the ISBFM also accelerates the convergence of the free surface profile with mesh refinement.

Both the ISBFM and the singular finite element method (SFEM) have advantages. They give similar results when rather coarse meshes are used. The SFEM is relatively simple to implement and does not require knowledge of the angular form of the local solution. However, unlike the SFEM, the ISBFM can be used with extensively refined meshes since the singular functions are independent of the refinement of the underlying mesh.

REFERENCES

1. L. G. Olson, G. C. Georgiou and W. W. Schultz, 'An efficient finite element method for treating singularities in Laplace's equation', *J. Comput. Phys.*, (1991), in press.
2. J. T. Oden and G. F. Carey, *Finite Elements. Mathematical Aspects, Vol. IV*, Prentice-Hall, Englewood Cliffs, NJ, 1983.
3. G. Strang and G. J. Fix, An Analysis of the Finite Element Method, Prentice-Hall, Englewood Cliffs, NJ, 1973.
4. G. C. Georgiou, L. G. Olson, W. W. Schultz and S. Sagan, 'A singular finite element for Stokes flow: the stick–slip problem', *Int. j. numer. methods fluids*, **9**, 1353–1367 (1989).
5. G. C. Georgiou, L. G. Olson and W. W. Schultz, 'Singular finite elements for the sudden-expansion and the die-swell problems', *Int. j. numer. methods fluids*, **10**, 357–371 (1990).
6. R. Keunings, 'On the high Weissenberg number problem', *J. Non-Newtonian Fluid Mech.*, **20**, 209–226 (1986).
7. G. G. Lipscomb, R. Keunings and M. M. Denn, 'Implications of boundary singularities in complex geometries', *J. Non-Newtonian Fluid Mech.*, **24**, 85–96 (1987).
8. W. J. Silliman and L. E. Scriven, 'Separating flow near a static contact line: slip at a wall and shape of a free surface', *J. Comput. Phys.*, **34**, 287–313 (1980).
9. D. H. Michael, 'The separation of a viscous liquid at a straight edge', *Mathematica*, **5**, 82–84 (1958).
10. H. K. Moffatt, 'Viscous and resistive eddies near a sharp corner', *J. Fluid Mech.*, **18**, 1–18 (1964).
11. H. Holstein and D. J. Paddon, 'A singular finite difference treatment of re-entrant corner flow', *J. Non-Newtonian Fluid Mech.*, **8**, 81–93 (1981).
12. G. C. Georgiou, L. G. Olson and W. W. Schultz, 'Two finite element methods for singularities in Stokes flow: the stick–slip problem', in T. J. Chung and G. R. Karr (eds.), *Finite Element Analysis in Fluids*, UAH Press, Huntsville, Al, 1989, pp. 992–997.
13. I. Babuška, 'The finite element method with Lagrangian multipliers', *Numer. Math.*, **20**, 179–192 (1973).
14. P. Hood, 'Frontal solution program for unsymmetric matrices', *Int. j. numer. methods eng.*, **10**, 379–399 (1976).
15. R. A. Walters, 'The frontal method in hydrodynamics simulations', *Comput. Fluids*, **8**, 265–272 (1980).
16. D. B. Ingham and M. A. Kelmanson, *Boundary Integral Equation Analyses of Singular, Potential and Biharmonic Problems*, Springer, Berlin, 1984.
17. G. C. Georgiou, 'Singular finite elements for Newtonian flow problems with stress singularities', *Ph.D. Thesis*, Department of Chemical Engineering, The University of Michigan, 1989.
18. W. W. Schultz and C. Gervasio, 'A study of the singularity in the die swell problem', *Q. J. Appl. Math. Mech.*, **43**, 407–425 (1990).
19. S. Richardson, A "stick–slip" problem related to the motion of a free jet at low Reynolds numbers', *Proc. Camb. Phil. Soc.*, **67**, 477–489 (1970).